The Oxidation of 2-Butene: A High Pressure Ignition Delay, Kinetic Modeling Study and Reactivity Comparison with Isobutene and 1-Butene

Yang Li [1], Chong-Wen Zhou[1], Kieran P. Somers[1], Kuiwen Zhang[1], Henry J. Curran*[,1]

[1]Combustion Chemistry Centre, National University of Ireland, Galway, Ireland

Abstract

Butenes are intermediates ubiquitously formed by decomposition and oxidation of larger hydrocarbons (e.g. alkanes) or alcohols present in conventional or reformulated fuels. In this study, a series of novel ignition delay time (IDT) experiments of trans-2-butene were performed in a high-pressure shock tube (HPST) and in a rapid compression machine (RCM) under conditions of relevance to practical combustors. This is the first IDT data of trans-2-butene taken at engine relevant conditions, and the combination of HPST and RCM results greatly expands the range of data available for the oxidation of trans-2-butene to higher pressures (10–50 atm), lower temperatures (670–1350 K) and a wide range of equivalence ratios (0.5–2.0). A comprehensive chemical kinetic mechanism has simultaneously been developed to describe the combustion of trans-2-butene. It has been validated using the IDT data measured here in addition to a large variety of literature data: jet-stirred reactor (JSR) speciation data, premixed flame speciation data, flow reactor speciation data and laminar flame speed data. Moreover, the reactivity of trans-2-butene is compared to that of the other two isomers, 1-butene and isobutene, and these comparisons are discussed. Important reactions are highlighted via flux and sensitivity analyses and help explain the differences in reactivity among the butene isomers.

---

* Corresponding author: henry.curran@nuigalway.ie

1. Introduction

Alkenes are important intermediates formed by the combustion of larger hydrocarbons, e.g., alkanes and alcohols. Moreover, liquefied petroleum gas (LPG) produced during oil refining contains significant amount of olefins, particularly propene and butenes [1], with gasoline fuel containing butenes, pentenes and hexenes in various amounts. Butene is the shortest alkene with structural isomers, namely 2-methylpropene (isobutene), which is a branched isomer, and 1-butene, cis-2-butene (c-2-C_4H_8) and tran-2-butene (t-2-C_4H_8), which are three linear isomers.

Recently, there have been some high-temperature and low-pressure experimental and kinetic modeling studies performed on trans-2-butene combustion, including pyrolysis and oxidation, speciation [2,3,4], flame speed [2,5], ignition temperature [5], etc., Table S1 of the Supplemental material. However, there is a lack of experimental data available in the literature at engine relevant, high-pressure and low-temperature, conditions. In addition, few studies have been specifically concerned with reactivity effects of the isomeric fuel structures.

In view of the above considerations, we have measured ignition delay times in a high-pressure shock tube (HPST) and in a rapid compression machine (RCM) under conditions of low temperatures (600–1000 K) and at high pressures (>10 atm), which are conditions of direct relevance with respect to gasoline, diesel, and low-temperature combustion (LTC) engine technologies. A comprehensive chemical kinetic mechanism to describe trans-2-butene oxidation has been developed including detailed low- and high-temperature reaction pathways specific to unsaturated fuel chemistry, and it is validated against the experimental results. An ignition reactivity comparison of three butene isomers (trans-2-butene, 1-butene and isobutene) has been performed, and a detailed chemical kinetic mechanism (AramcoMech 2.0) has been developed to explain the reactivity differences which account for the isomeric structure effects on ignition/reactivity properties.

2. Experiment

Experiments were performed in the NUI Galway HPST and RCM facilities as described previously [6,7]. All fuels were acquired from Sigma Aldrich at 99.5% purity. Oxygen, nitrogen, argon and carbon dioxide were acquired from BOC Ireland at high purity (≥99.5%).

Table 1 shows that identical experimental conditions at $\varphi = 1.0$ for cis- and tran-2-butene were selected ($p = 10$, 30 and 50 atm), and Fig. 1 shows the IDT measurements for these two isomers and they are identical. Therefore, they will be named as 2-butene in the following text. Typical pressure-time traces and original experimental data are shown in the Supplemental material, Fig. S1 and Table S3–S17.

Table 1. Detailed mixture compositions (%).

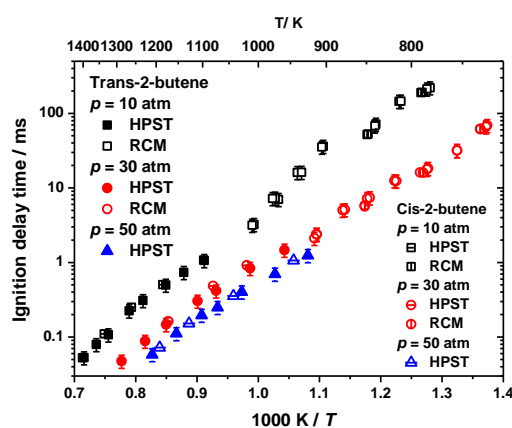|	Fuel	O_2	Diluent	φ
	1.72	20.64	77.64	0.5
t-2-C_4H_8	3.38	20.29	76.33	1.0
	6.54	19.63	73.83	2.0
c-2-C_4H_8	3.38	20.29	76.33	1.0

Figure 1. IDT measurements for trans/cis-2-butene at $\varphi = 1.0$ and $p = 10$, 30, 50 atm.

3. Results and Discussions

3.1. Chemical kinetic mechanism development

The current mechanism development is based on the H_2/O_2 sub-mechanism from Kéromnès et al. [8], the C_1–C_2 AramcoMech 1.3 sub-mechanism [9] and the propene/allene/propyne sub-mechanism adopted from Burke et al. [10,11]. Thermodynamic parameters are estimated using the group additivity method employed by Benson [12] with updated group values by Burke et al. [13] as utilized in THERM [14].

During these developments, the mechanism has been validated against numerous experimental conditions and targets. Key reactions for 2-butene oxidation at different temperature and pressure conditions are highlighted using sensitivity and flux analyses for ignition times. The 2-butene combustion chemistry model developed in this work has improved the predictions against a variety of experimental results. The comprehensive kinetic mechanism, thermochemistry, transport files and molecular structure glossary are provided as Supplemental material. In addition, speciation measurements in a JSR [2], laminar flame speeds [2] and ignition temperature measurements [5] shown in the Supplemental material, Fig. S3–S8 also indicates that both isomers (cis- and trans-2-butene) exhibit identical reactivity.

3.2. Important reaction classes highlighted

All simulations, including brute force sensitivity analyses [15] were performed using CHEMKIN-PRO [16]. Figure 2 highlights the important reactions controlling 2-butene oxidation for a series of representative conditions: $\varphi = 1.0$, $T = 1250$ K, 950 K and 700 K, $p = 30$ atm.

The choice of rate constants for many of the important reactions highlighted above are discussed and explained in Sections 3.4.3 and 3.4.4. The Arrhenius coefficients for all of the important reactions are provided in Table S2 of the Supplemental material. The performance of the mechanism presented in this study is compared with the performance of selected mechanisms available in the literature [2,3,5], comparisons of which are provided in Figs. S12 and S13 of the Supplemental material. It was found that existing literature mechanisms were unable to simulate our new

experimental data at these relatively high-pressure, low-temperature conditions, as they did not include the low-temperature chemistry reactions necessary to describe fuel oxidation in this range.
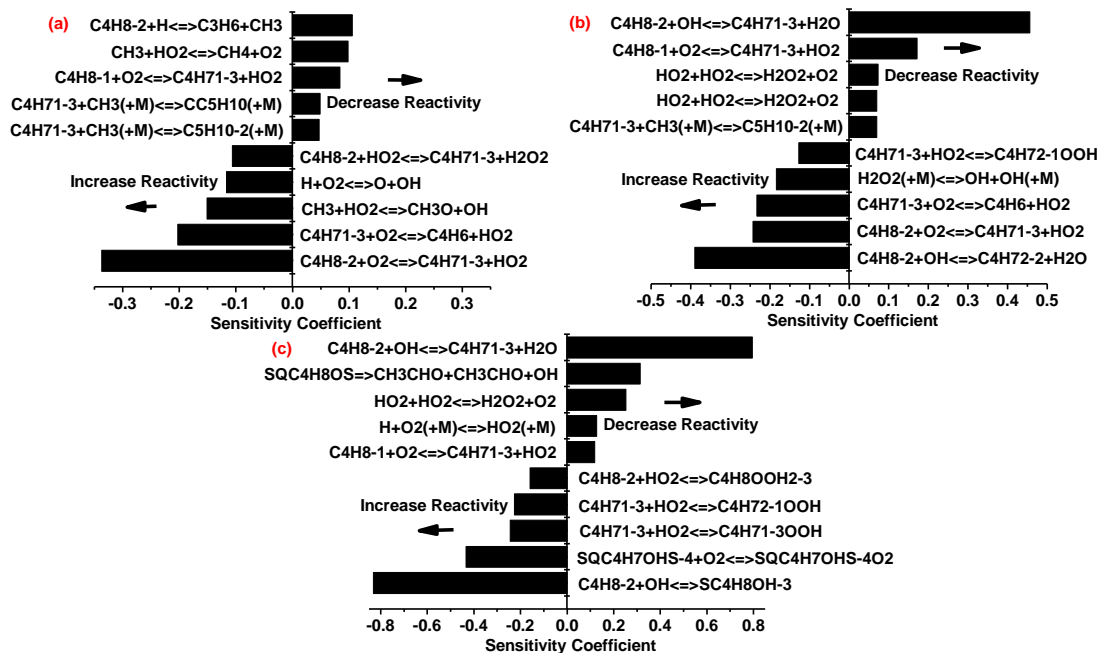
Figure 2. Sensitivity analyses for 2-butene, $\phi = 1.0$, $p = 30$ atm. (a) $T = 1250$ K, (b) $T = 950$ K, (b) $T = 700$ K.

3.3. Flux analyses

Flux analyses were carried out under the same conditions as the sensitivity analyses: $\varphi = 1.0$ in 'air' (O_2 : $N_2 = 21$: 79), $p = 30$ atm, $T = 700$ K, 950 K and 1250 K and at 20% fuel consumed, these being most representative for the experimental conditions studied, Fig. 3. These analyses cover the most common reactions occurring at the various temperature regimes, and for brevity, any reaction paths representing <5% flux have been excluded.
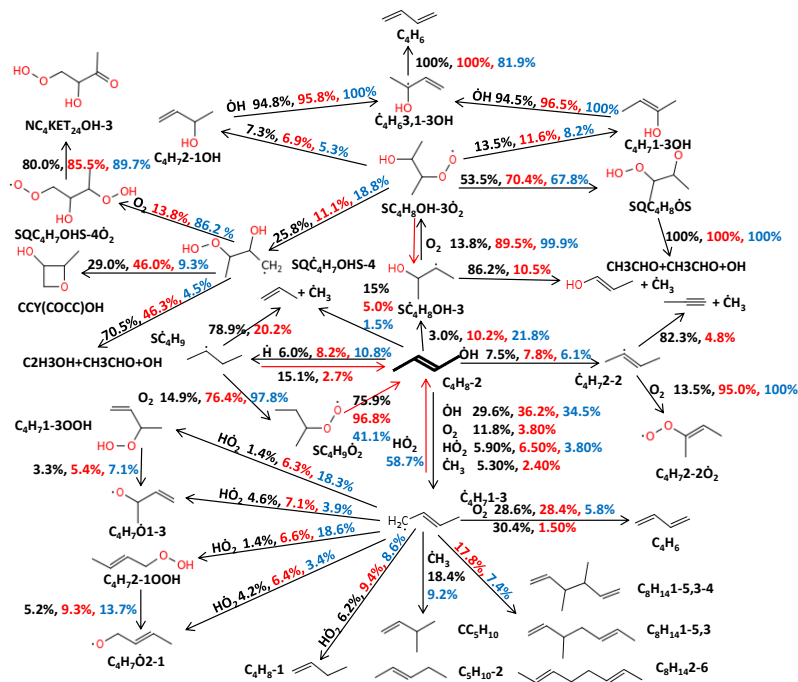
Figure 3. Flux analysis for 2-butene oxidation at $\varphi = 1.0$, 30 atm and 20% fuel consumption. Black numbers: 1250 K; red numbers: 950 K; blue numbers: 700 K.

3.4. Model Validation

Figures 4–6 show both our experimental data and model simulations for all mixtures. Solid symbols represent experimental data obtained in the HPST, open symbols represent experiments taken in the RCM. Solid lines correspond to IDTs calculated via constant-volume, adiabatic simulations. Dashed lines represent IDTs calculated using effective volume histories from the RCM to account for facility effects as discussed previously [15].

3.4.1. Influence of pressure on ignition delay time

Figure 4 shows the effect of pressure on ignition times obtained in both the HPST and in the RCM for fuel/air mixtures at $\varphi = 0.5$, 1.0 and 2.0. The experimental results show that reactivity increases with increasing pressure at all equivalence ratios. As the pressure increases so does the absolute concentration of reactants, resulting in the observed increase in reactivity. The mechanism is able to predict this effect over a wide range of pressures, temperatures and equivalence ratios.
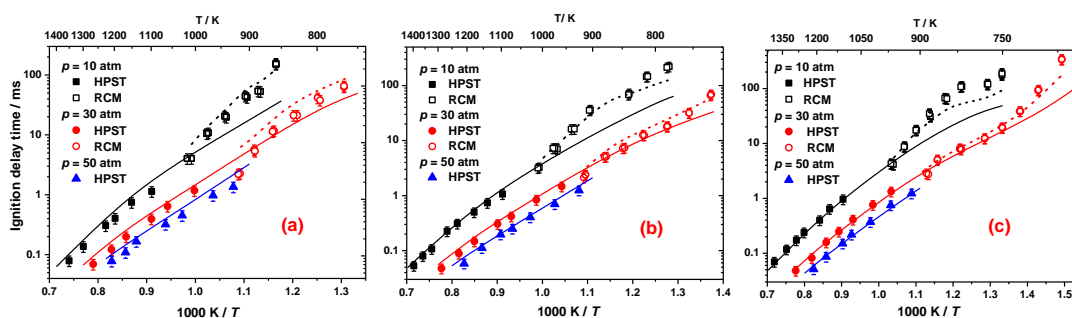

Figure 4. Influence of pressure on 2-butene IDTs. (a) $\varphi = 0.5$, (b) $\varphi = 1.0$, (c) $\varphi = 2.0$.

3.4.2. Influence of equivalence ratio on ignition delay time

Ignition delay times were measured at three fuel/air mixture equivalence ratios of 0.5, 1.0 and 2.0 at 10, 30 and 50 atm, Fig. 5. In the range of conditions studied here, fuel-rich mixtures are fastest to ignite with fuel-lean mixtures being slowest. This is due to an increased concentration of fuel, as the chemistry based on the 2-butanol-3-yl radical, $S\dot{C}_4H_8OH\text{-}3$, which is generated from the addition of hydroxyl radical to the C=C double bond, dominates reactivity, as discussed in the section on temperature effects on ignition times. Again, the model shows good agreement across the entire temperature and pressure ranges.

At low to intermediate temperatures (~700–1000 K) fuel-rich mixtures ignite faster than fuel-lean ones. This behavior at low temperatures is due to an increase in fuel concentration, as the chemistry of the fuel radicals forms the kinetic bottleneck and has the largest effect on ignition delay times.

The difference in IDTs between the mixtures is much smaller at high temperatures (1000–1300 K) relative to that at low and intermediate temperatures. However, based on the relative slopes of the

data, all datasets would appear to converge with increasing temperature, as has been observed and discussed previously [15].
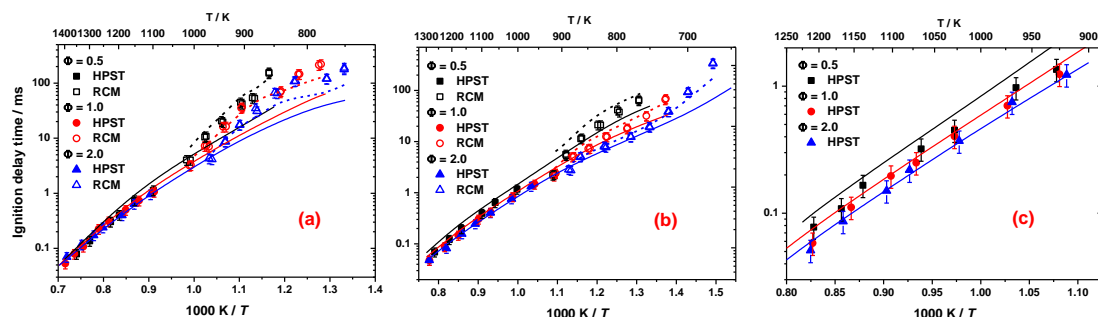

Figure 5. Influence of equivalence ratio on 2-butene IDTs. (a) p = 10 atm, (b) p = 30 atm, (c) p = 50 atm.

3.4.3. Influence of temperature on ignition delay time

Based on the sensitivity and flux analysis results at high temperature (T = 1250 K) shown in Fig. 2 (a) and Fig. 3 (black numbers), H-atom abstraction by molecular oxygen from allylic carbon atoms which result in the generation of 1-buten-3-yl radicals ($\dot{C}_4H_7$1-3) and their subsequent reaction with molecular oxygen ($\dot{C}_4H_7$1-3 + O_2 ↔ C_4H_6 + $H\dot{O}_2$) are the most promoting reactions. It is worth nothing that the reaction $\dot{C}_4H_7$1-3 + O_2 ↔ C_4H_6 + $H\dot{O}_2$ is not chemically activated via the sequence: $\dot{R}$ + O_2 ↔ $R\dot{O}_2$ ↔ alkene + $H\dot{O}_2$, instead being a direct abstraction. The well depth of the association reaction $\dot{C}_4H_7$1-3 + O_2 ↔ $C_4H_7$1-3$\dot{O}_2$ has been calculated here to be 19.93 kcal/mol using Gaussian 09 [17] and the composite CBS-QB3 method. The barrier for the subsequent concerted elimination of hydroperoxyl radical is 27.18 kcal/mol, so the reverse reaction to $\dot{C}_4H_7$1-3 + O_2 is kinetically favored over the formation of C_4H_6 + $H\dot{O}_2$. Alternatively, the formation of C_4H_6 + $H\dot{O}_2$ via chemically activated complexes via a direct H-atom abstraction from the primary carbon side is plausible, and the rate constant is adopted from the theoretical work of DeSain et al. [18]. The most inhibiting reaction is the chemically activated reaction C_4H_8-2 + $\dot{H}$ ↔ C_3H_6 + $\dot{C}H_3$, the rate constant of which is calculated here on the $\dot{C}_4H_9$ potential energy surface at the CCSD(T)/cc-pvXZ//M062X/6-311++G(d,p) level of theory (where X = D, T and Q) and extrapolated to the

8

complete basis set (CBS) limit [19,20]. This reaction results in the consumption of atomic hydrogen, competing with $\dot{H} + O_2 \leftrightarrow \ddot{O} + \dot{O}H$, which controls reactivity at high temperatures.

At intermediate temperatures ($T = 950$ K) the two most sensitive and competitive reactions, Fig. 2 (b), are allylic-hydrogen abstraction reactions, which result in the generation of $\dot{C}_4H_71$-3 radical, and hydrogen atom abstractions from secondary vinylic carbon atom which results in the generation of 2-buten-2-yl radical ($\dot{C}_4H_72$-2). This promoting/inhibiting effect appears to be linked to the ease-of-oxidation of these respective radicals. As shown in flux analysis results in Fig. 3 (red numbers), $\dot{C}_4H_71$-3 radical is resistant to oxidation by O_2, and is consumed subsequently by a) chain propagating reactions with hydroperoxyl radical resulting in methyl-allyl-hydroperoxide (C_4H_71-3OOH, C_4H_72-1OOH), methyl-allyl-oxy ($C_4H_7\dot{O}1$-3, $C_4H_7\dot{O}2$-1) and hydroxyl radicals (in a 50:50 ratio); b) chain termination reactions with methyl radicals resulting in the formation of 2-pentene (C_5H_{10}-2) and 3-methyl-1-butene (CC_5H_{10}) (with an assumed 50:50 branching ratio). On the contrary, 2-buten-2-yl radicals ($\dot{C}_4H_72$-2) react with molecular oxygen producing atomic oxygen, methyl ketene and methyl radicals in chain-branching sequence.

At lower temperatures ($T = 700$ K) shown in Fig. 2 (c), again, the most inhibiting reaction is hydrogen abstraction reactions by hydroxyl radicals from allylic carbon atom (C_4H_8-1 + $\dot{O}H \leftrightarrow \dot{C}_4H_71$-3 + H_2O), because it results in the consumption of a reactive hydroxyl radical and the formation of a resonantly stabilized 1-butenyl-3-yl radical ($\dot{C}_4H_71$-3) radical. The addition of hydroxyl radical to C=C double bond forming $S\dot{C}_4H_8OH$-3 radical pronouncedly promotes reactivity. Based on flux analysis results in Fig. 3 (blue numbers), the reason being that: chain branching can subsequently occur from the addition of O_2 to the 2-butene + $\dot{O}H$ adduct, isomerization and second O_2 addition, with the decomposition of the nascent ketohydroperoxide ultimately promoting reactivity via generation of $\dot{O}H$ radicals.

It is also worth noting that, at all temperatures presented in Fig. 2, the reaction C_4H_8-1 + $O_2 \leftrightarrow \dot{C}_4H_71$-3 + $H\dot{O}_2$ always ranks among the top five most sensitive reactions inhibiting reactivity. As we can see from flux analysis results in Fig. 3, this is because the reaction between $\dot{C}_4H_71$-3 and $H\dot{O}_2$

radicals results in the formation of two stable species. Note also that the $\dot{C}_4H_7$1-3 radical is generated in the oxidation of 1-butene, and thus both the 1- and 2-butene oxidation mechanisms are intrinsically linked and need to be generated simultaneously.

3.4.4. *Influence of isomeric structure on ignition delay time*

The effect of isomeric structure on ignition delay times for three butene isomers (iso-, 1-, and 2-butene) are compared, Fig. 6. Representative conditions have been selected: (a) $\varphi = 0.5$, $p = 10$ atm, (b) $\varphi = 1.0$, $p = 30$ atm, (c) $\varphi = 2.0$, $p = 50$ atm. It is shown that 1-butene is the fastest to ignite, followed by 2-butene, with isobutene being the slowest at all equivalence ratios and pressures and throughout the entire temperature range.
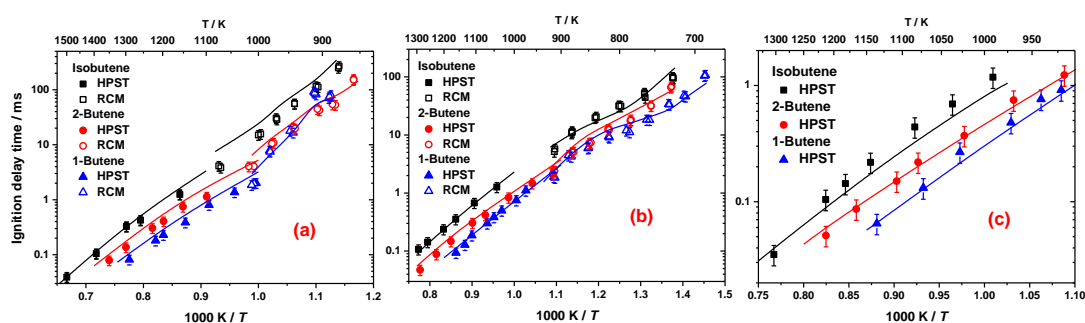

Figure 6. Influence of isomeric structure on 2-butene IDTs. (a) $\varphi = 0.5$, $p = 10$ atm, (b) $\varphi = 1.0$, $p = 30$ atm, (c) $\varphi = 2.0$, $p = 50$ atm.

In order to explain the differences in reactivity due to isomeric structure, sensitivity analyses for 1-, 2-butene and isobutene oxidation have been carried out at identical conditions: $\varphi = 1.0$, $T = 1250$ K, 950 K and 700 K, $p = 30$ atm, shown in Fig. S2 of the Supplemental material. H-atom abstraction reactions by hydroxyl radicals from an allylic carbon atom inhibit reactivity for all three isomers at all temperatures. The rate constants of C_4H_8-1 + $\dot{O}H$ and C_4H_8-2 + $\dot{O}H$ are adopted from the experimental work and theoretical study of Vasu et al. [21] at the CCSD(T)/6-311++G(d,p)//QCISD/6-31G(d)) level of theory, while the rate constant of iC_4H_8 + $\dot{O}H$ is calculated at the QCISD(T)/CBS//M062X/6-311++G(d,p) level of theory as part of this study. Figure 7 (a) shows a comparison of these three rates constants at high temperatures (1000–2000 K). The rate constant of iC_4H_8 + $\dot{O}H$ is faster than that of C_4H_8-2 + $\dot{O}H$, with C_4H_8-1 + $\dot{O}H$ being the slowest,

which means the reactivity of isobutene is inhibited the most by this reaction, followed by 2-butene and 1-butene.

At high temperatures (>1000 K), the most promoting reactions are H-atom abstraction reactions by molecular oxygen from allylic carbon atom which results in the generation of methyl-allyl radicals ($i\dot{C}_4H_7$ and $\dot{C}_4H_71$-3). The rate constants of $iC_4H_8 + O_2$ is adopted from Yasunaga et al. [22], while the rate constants of C_4H_8-1 + O_2 and C_4H_8-2 + O_2 are determined by the Evans-Polanyi relationship developed by Somers et al. [23]. Figure 7 (b) shows a comparison of these three rates constants, with the rates of C_4H_8-1 + O_2 and C_4H_8-2 + O_2 being faster than that of $iC_4H_8 + O_2$, which means the reactivity of 1-butene and 2-butene are promoted more than isobutene. Moreover, the subsequent reaction $\dot{C}_4H_71$-3 + O_2 ↔ $C_4H_6 + H\dot{O}_2$ promotes reactivity more for both 1-butene and 2-butene but this reaction doesn't exist for isobutene.

The most inhibiting reactions for 1- and 2-butene oxidation are $\dot{H}$ atom addition reactions to the fuel on the same potential energy surface. Addition to the terminal carbon atom on 1-butene and non-terminal addition to 2-butene both generate propene and a methyl radical with rate constant comparisons shown in Fig. 7 (c). The rate of addition to 2-butene is faster than for 1-butene at high temperatures, inhibiting the reactivity of 2-butene more than 1-butene. Moreover, addition to the non-terminal carbon in 1-butene results in the formation of $C_2H_4 + \dot{C}_2H_5$, which ultimately generates two vinyl radicals and a hydrogen atom, promoting reactivity.

At intermediate temperatures (~800–1000 K), unlike isobutene, both 1- and 2-butene can undergo H-atom abstraction by hydroxyl radicals from secondary vinylic carbon atom resulting in the generation of 1-buten-2-yl ($\dot{C}_4H_71$-2) and 2-buten-2-yl ($\dot{C}_4H_72$-2) radicals, and their subsequent reactions with molecular oxygen generates alkenylperoxy radicals, C_4H_71-2$\dot{O}_2$ and C_4H_72-2$\dot{O}_2$, followed by O–O bond fission resulting in $\ddot{O}$ atoms, a sequence which pronouncedly promotes reactivity. However, the β-scission of 2-butanone-3-yl ($C_4H_7\dot{O}2$-2) radical, generated via O–O bond fission of a C_4H_72-2$\dot{O}_2$ radical, generates methyl radicals which can recombine with $\dot{C}_4H_71$-3 radicals to produce 2-pentene and 3-methyl-1-butene, which slightly inhibits reactivity.

At low temperatures (<800 K), the promoting reactions for the three fuels changes from H-atom abstraction to hydroxyl radical addition to the C=C double bond. Rate constants are compared in Fig. 7 (d), and are estimated by analogy to propene plus $\dot{O}H$ radical as calculated by Zádor et al. [24] (with 75:25 branching ratio for terminal verses central addition for both isobutene and 1-butene [25]), hence the total rate constant of the reaction C_4H_8-2 + $\dot{O}H$ is 2.5 times slower than that of isobutene and 1-butene. Furthermore, the butanol-alkyl ($S\dot{C}_4H_8OH$-3, $P\dot{C}_4H_8OH$-2, $S\dot{C}_4H_8OH$-1, $I\dot{C}_4H_8OH$-IT and $I\dot{C}_4H_8OH$-TI) radicals generated can react with molecular oxygen followed by an isomerization reaction to form hydroperoxyl-alkyl radicals (QOOH). However, because of the isomeric structural difference between 1-butene and isobutene, 1-butene oxidation facilitates more chain branching reactions than isobutene leading to more rapid chain branching in 1-butene compared to isobutene.
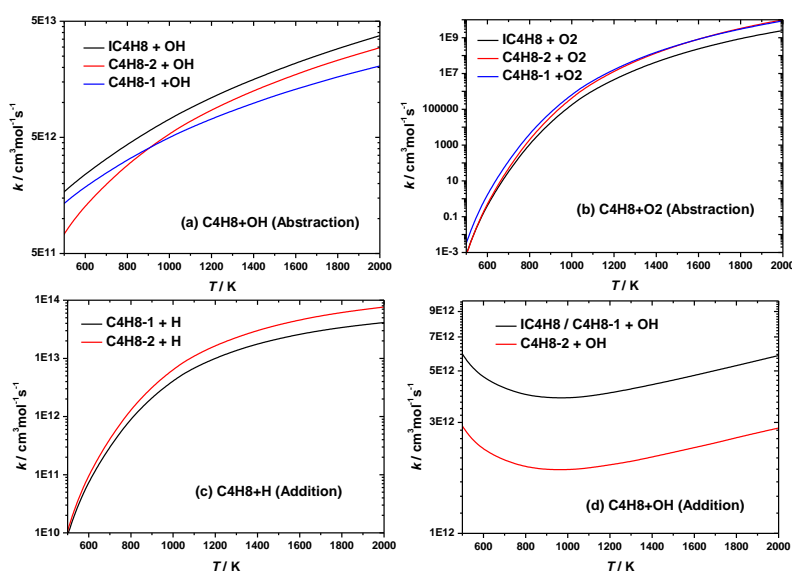

Figure 7. Rate constants comparison for isobutene, 2-butene and 1-butene mechanism.

4. Conclusions

This work represents the first ignition delay study of 2-butene oxidation at elevated pressures in a HPST and in a RCM over a wide range of pressures, temperatures and equivalence ratios. The results presented greatly expand the ignition delay time database available for mechanism validation for 2-butene oxidation. Further, the ignition reactivity of the three butene isomers (1-, 2- and isobutene) has been compared under the same conditions.

It was found that an increase in reflected shock pressure resulted in shorter ignition delay times (higher reactivity) for all equivalence ratios investigated, which is typical of the influence of pressure on fuel reactivity. The effect of equivalence ratio on ignition delay times depended on the temperature of the experiment, where all mixtures had similar reactivity at higher temperatures and fuel-rich mixtures were most reactive at lower temperatures. As to the effect of isomeric structure on ignition delay times for three butene isomers, 1-butene is the fastest to ignite, followed by 2-butene, with isobutene being the slowest.

A detailed chemical kinetic mechanism has been developed to describe the combustion of 2-butene, it includes comprehensive low- and high-temperature reaction pathways specific to unsaturated fuel chemistry. Important reactions were identified through sensitivity and flux analyses. Rate constants have been adopted from experimental and theoretical studies where possible. However, for reactions where the literature is lacking, rate constants were calculated from *ab initio* methods or estimated. The mechanism is validated against our new experiments and relevant literature data. The current mechanism captures well most of the experimental results of ignition delay times, as well as the flame speeds, speciation results from premixed flame and flow reactor results from the literature.

This is also the first study that explains the reactivity difference between the three butene isomers using detailed chemistry at these relatively high-pressure, low-temperature conditions. Together with recent studies on ethylene [26,27], propene [10,11], isobutene [28] and 2-methyl-2-butene [29], a consistent and detailed picture of low-temperature vinylic and allylic hydrocarbon combustion

kinetics is starting to emerge to supplement our recently re-developed rate rules for *n-* and *iso-*alkanes [30]. Future research efforts will be focused on: a) reaction class development for unsaturated hydrocarbons, and b) rate rules for important reaction classes.

References

[1] K. Morganti PhD thesis, A Study of the Knock Limits of Liquefied Petroleum Gas (LPG) in Spark-Ignition Engines, The University of Melbourne, 2003.

[2] Y. Fenard, P. Dagaut, G. Dayma, F. Halter, F. Foucher, Proc. Combust. Inst. 35 (2015) 317–324.

[3] M. Schenk, L. Leon, K. Moshammer, P. Obwald, T. Zeuch, L. Seidel, F. Mauss, K. Kohse-Hoinghaus, Combust. Flame 160 (2013) 487–503.

[4] Y. Zhang, J. Cai, L. Zhao, J. Yang, H. Jin, Z. Cheng, Y. Li, L. Zhang, F. Qi, Combust. Flame 159 (2012) 905–917.

[5] P. Zhao, W. Yuan, H. Sun, Y. Li, A. P. Kelley, X. Zheng, C. K. Law, Proc. Combust. Inst. 35 (2015) 309–316.

[6] D. Darcy, C.J. Tobin, K. Yasunaga, J.M. Simmie, J. Würmel, W.K. Metcalfe, T. Niass, S.S. Ahmed, C.K. Westbrook, H.J. Curran, Combust. Flame 159 (7) (2012) 2219–2232.

[7] D. Darcy, H. Nakamura, C.J. Tobin, M. Mehl, W.K. Metcalfe, W.J. Pitz, C.K. Westbrook, H.J. Curran, Combust. Flame 161 (1) (2014) 65–74.

[8] A. Keromnes; W. K. Metcalfe; K. A. Heufer; N. Donohoe; A. K. Das; C. J. Sung; J. Herzler; C. Naumann; P. Griebel; O. Mathieu; M. C. Krejci; E. L. Petersen; W. J. Pitz; H. J. Curran, Combust. Flame 160 (6) (2013) 995-1011.

[9] W. K. Metcalfe; S. M. Burke; S. S. Ahmed; H. J. Curran, Int. J. Chem. Kinet. 45 (10) (2013) 638-675.

[10] S. M. Burke; U. Burke; R. Mc Donagh; O. Mathieu; I. Osorio; C. Keesee; A. Morones; E. L. Petersen; W. J. Wang; T. A. DeVerter; M. A. Oehlschlaeger; B. Rhodes; R. K. Hanson; D. F. Davidson; B. W. Weber; C. J. Sung; J. Santner; Y. G. Ju; F. M. Haas; F. L. Dryer; E. N. Volkov; E. J. K. Nilsson; A. A. Konnov; M. Alrefae; F. Khaled; A. Farooq; P. Dirrenberger; P. A. Glaude; F. Battin-Leclerc; H. J. Curran, Combust. Flame 162 (2) (2015) 296-314.

[11] S. M. Burke; W. Metcalfe; O. Herbinet; F. Battin-Leclerc; F. M. Haas; J. Santner; F. L. Dryer; H. J. Curran, Combust. Flame 161 (11) (2014) 2765–2784.

[12] S. W. Benson, Thermochemical kinetics, Wiley, 1976.

[13] S. M. Burke; J. M. Simmie; H. J. Curran, J. Phys. Chem. Ref. Data 44 (1) (2015) 013101.

[14] E. R. Ritter; J. W. Bozzelli, Int. J. Chem. Kinet. 23 (9) (1991) 767–778.

[15] W.K. Metcalfe, S.M. Burke, S.S. Ahmed, H.J. Curran, A Hierarchical and Comparative Kinetic Modeling Study of C1 − C2 Hydrocarbon and Oxygenated Fuels, Int. J. Chem. Kinet. 45 (2013) 638-675.CHEMKIN-PRO 15131, Reaction Design, San Diego, 2010

[16] M. J. Frisch, G. W. Trucks, H. B. Schlegel, G. E. Scuseria, M. A. Robb, J. R. Cheeseman, G. Scalmani, V. Barone, B. Mennucci, G. A. Petersson, Gaussian 09, revision A.02; Gaussian, Inc.: Wallingford CT, 2009.

[17] J. D. DeSain, S. J. Klippenstein, J. A. Miller, and C. A. Taatjes, J. Phys. Chem. A 2003, 107, 4415–4427.

[18] J. M. L. Martin, Chem. Phys. Lett. 259 (5-6) (1996) 669–678.

[19] D. Feller; D. A. Dixon, J. Chem. Phys. 115 (8) (2001) 3484–3496.

[20] S. S. Vasu, L. K. Huynh, D. F. Davidson, R. K. Hanson, D. M. Golden, J. Phys. Chem. A 2011, 115, 2549–2556.

[21] K. Yasunaga; Y. Kuraguchi; R. Ikeuchi; H. Masaoka; O. Takahashi; T. Koike; Y. Hidaka, Proc. Combust. Inst. 32 (2009) 453–460.

[22] K.P. Somers, J.M. Simmie, F. Gillespie, C. Conroy, G. Black, W.K. Metcalfe, F. Battin-Leclerc, P. Dirrenberger, O. Herbinet, P.-A. Glaude, P. Dagaut, C. Togbe, K. Yasunaga, R.X. Fernandes, C. Lee, R. Tripathi, H.J. Curran, Combust. Flame (2013) 160 2291–2318.

[23] J. Zádor, A. W. Jasper, J. A. Miller, Phys. Chem. Chem. Phys. 11 (46) (2009) 11040–11053.

[24] J. C Loison, J. Daranlot, A. Bergeat, F. Caralp, R. Mereau, K.M. Hickson, J. Phys. Chem. A 114 (2010) 13326–13336.

[25] M.M. Kopp, N.S. Donato, E.L. Petersen, W.K. Metcalfe, S.M. Burke, H.J. Curran, J. Prop. Power (2014) 30(3) 799–811.

[26] M.M. Kopp, N.S. Donato, E.L. Petersen, W.K. Metcalfe, S.M. Burke, H.J. Curran, J. Prop. Power (2014) 30(3) 790–798.

[27] C. Zhou, Y. Li, E. O'Connor, K. P. Somers, S. Thion, C. Keesee, O. Mathieu, E. L. Petersen, T. A. DeVerter, M. A. Oehlschlaeger, G. Kukkadapu, C. Sung, M. Alrefae, F. Khaled, A. Farooq, P. Dirrenberger, P. Glaude, F. Battin-Leclerc, J. Santner, Y. Ju, T. Held, F. M. Haas, F. L. Dryer, H. J. Curran, Combust. Flame, 2016, 167, 353-379.

[28] C.K. Westbrook, W.J. Pitz, M. Mehl, P-A. Glaude, O. Herbinet, S. Bax, F. Battin-Leclerc, O. Mathieu, E.L. Petersen, J. Bugler, H.J. Curran, J. Phys. Chem. A (2015) 119(28) 7462–7480.

[29] J. Bugler, K. P. Somers, E. J. Silke, and H. J. Curran, J. Phys. Chem. A 2015, 119, 7510−7527.